An Ultra-Broad-Band Reflection-Type Phase-Shifter MMIC With Series and Parallel *LC* Circuits

Kenichi Miyaguchi, *Member, IEEE*, Morishige Hieda, *Member, IEEE*, Kazuhiko Nakahara, *Member, IEEE*, Hitoshi Kurusu, Masatoshi Nii, Michiaki Kasahara, Tadashi Takagi, *Member, IEEE*, and Shuji Urasaki, *Senior Member, IEEE*

***Abstract*—An ultra-broad-band reflection-type phase shifter is proposed. Theoretically, the proposed phase shifter has frequency-independent characteristics in the case of 180° phase shift. The phase shifter is composed of a 3-dB hybrid coupler and a pair of novel reflective terminating circuits. The reflective terminating circuit switches two states of series and parallel *LC* circuits. Using an ideal circuit model without parasitic circuit elements, we have derived the determining condition of frequency independence of circuit elements. Extending the concept, we can also obtain a broad-band phase shifter for other phase difference as well. In this case, for a given phase difference and an operating frequency, we also derive a condition to obtain minimum variation of phase difference around the operating frequency. This enables the broad-band characteristics for arbitrary phase difference. The fabricated 180° reflective terminating circuit monolithic microwave integrated circuit (MMIC) has achieved a phase difference of 183°±3° over 0.5–30 GHz. The 180° phase-shifter MMIC has demonstrated a phase shift of 187°±7° over 0.5–20 GHz. The 90° reflective terminating circuit MMIC has performed a phase difference of 93° ±7° over 4–12 GHz.**

***Index Terms*—Broad-band, MMIC, monolithic microwave integrated circuit, phase shifter, reflection type.**

I. Introduction

PHASE shifters have been widely used in active phased-array antennas (APAAs) for electronic beam steering [1]. Recently, broad-band APAAs have been required in wide-band microwave applications. According to the demand of wide-band APAAs, broad-band phase shifters have been developed [2]–[5]. In this paper, we propose an ultra-broad-band reflection-type phase shifter with new reflective terminating circuits. The conventional reflection-type phase shifter, which consists of a 3-dB hybrid coupler and a pair of reflective terminating circuits with impedance transformers, is able to be operated in a relatively wide frequency range. However, it still has a restriction of operating bandwidth because of poor frequency characteristics of the impedance transformers [6].

Manuscript received March 30, 2001; revised August 21, 2001.

K. Miyaguchi, M. Hieda, M. Kasahara, T. Takagi, and S. Urasaki are with the Information Technology Research and Development Center, Mitsubishi Electric Corporation, Kamakura 247-8501, Japan.

K. Nakahara is with Kamakura Works, Mitsubishi Electric Corporation, Kamakura 247-8520, Japan.

H. Kurusu is with the High Frequency and Optical Semiconductor Division, Mitsubishi Electric Corporation, Itami 664-8641, Japan.

M. Nii is with the Communication Systems Center, Mitsubishi Electric Corporation, Amagasaki 661-8661, Japan.

Publisher Item Identifier S 0018-9480(01)10444-8.

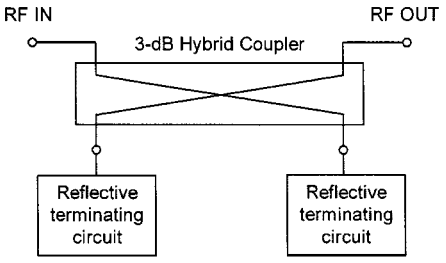

Fig. 1. Schematic diagram of a reflection-type phase shifter.

The proposed phase shifter is composed of a broad-band 3-dB hybrid coupler and a pair of novel reflective terminating circuits. Theoretically, it has frequency-independent characteristics in the case of 180° phase shift. The reflective terminating circuit switches two states of series and parallel *LC* circuits. Using an ideal circuit model without parasitic circuit elements, we have derived the determining condition of frequency independence of circuit elements. Extending the concept, we can also obtain a broad-band phase shifter for other phase difference as well. In this case, for a given phase difference and an operating frequency, we also derive a condition to obtain minimum variation of phase difference around the operating frequency. This enables the broad-band characteristics for arbitrary phase difference. The 180° and 90° reflective terminating circuits' monolithic microwave integrated circuit (MMIC) and the 180° reflection-type phase-shifter MMIC have been designed and fabricated by 0.5-μm pseudomorphic high electron-mobility transistor (pHEMT) MMIC technology. The 180° reflective terminating circuit MMIC has achieved a phase difference of 183°±3° over 0.5–30 GHz. The 180° phase-shifter MMIC has demonstrated a phase shift of 187°±7° over 0.5–20 GHz. The 90° reflective terminating circuit MMIC has performed a phase difference of 93°±7° over 4–12 GHz.

II. Novel Reflective Terminating Circuit

A. 180° Phase-Difference Case

Fig. 1 shows a schematic diagram of a reflection-type phase shifter. It consists of a broad-band 3-dB hybrid coupler and a pair of reflective terminating circuits. Fig. 2 shows a schematic diagram of a novel reflective terminating circuit. L_S and C_S correspond to inductor and capacitor of the series *LC* circuit, while L_P and C_P are the inductance and capacitance of the parallel *LC* circuit, respectively. The reflective terminating circuit switches series and parallel *LC* circuits by switching the circuit.

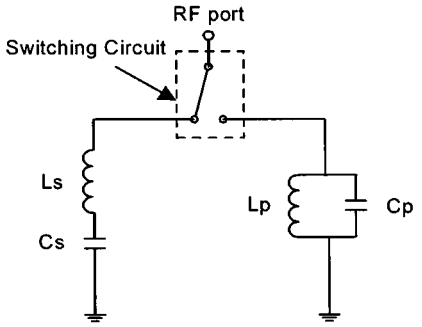

Fig. 2. Schematic diagram of a novel reflective terminating circuit.

Reflection coefficients Γ_S and Γ_P of series and parallel *LC* circuits are given by

$$\Gamma_S = |\Gamma_S| e^{j\phi_S} = \frac{Z_S - Z_0}{Z_S + Z_0} \tag{1}$$

$$\Gamma_P = |\Gamma_P| e^{j\phi_P} = \frac{Z_P - Z_0}{Z_P + Z_0} \tag{2}$$

where

$$Z_S = j\omega L_S + \frac{1}{j\omega C_S} \tag{3}$$

$$Z_P = \frac{1}{\dfrac{1}{j\omega L_P} + j\omega C_P}. \tag{4}$$

In (1)–(4), Z_S and Z_P are the impedance of series and parallel *LC* circuits and ϕ_S and ϕ_P are the reflection phase of series and parallel *LC* circuits, respectively. Z_0 is the impedance of a 3-dB hybrid coupler. Using (1) and (2), ϕ_S and ϕ_P can be written as

$$\phi_S = \tan^{-1} \frac{2Z_0 \left(\omega L_S - \dfrac{1}{\omega C_S}\right)}{\left(\omega L_S - \dfrac{1}{\omega C_S}\right)^2 - Z_0^2} \tag{5}$$

$$\phi_P = \tan^{-1} \frac{2Z_0 \left(\dfrac{1}{\omega L_P} - \omega C_P\right)}{1 - Z_0^2 \left(\dfrac{1}{\omega L_P} - \omega C_P\right)^2}. \tag{6}$$

The phase difference ϕ is defined by the following equation:

$$\begin{aligned}\phi &= \phi_S - \phi_P \\ &= \tan^{-1} \frac{2Z_0 \left(\omega L_S - \dfrac{1}{\omega C_S}\right)}{\left(\omega L_S - \dfrac{1}{\omega C_S}\right)^2 - Z_0^2} \\ &\quad - \tan^{-1} \frac{2Z_0 \left(\dfrac{1}{\omega L_P} - \omega C_P\right)}{1 - Z_0^2 \left(\dfrac{1}{\omega L_P} - \omega C_P\right)^2}.\end{aligned} \tag{7}$$

In order to obtain broad-band phase difference characteristics, ϕ has to satisfy the following condition for all frequencies:

$$\frac{d\phi}{d\omega} \equiv 0, \qquad \text{for all } \omega. \tag{8}$$

Substituting (7) into (8), we can obtain the following polynomial equation:

$$\begin{aligned}&L_P(1+\omega^2 L_S C_S)\left[1 + Z_0^2\left(\frac{1}{\omega L_P} - \omega C_P\right)^2\right] \\ &\quad - C_S(1+\omega^2 L_P C_P)\left[\left(\omega L_S - \frac{1}{\omega C_S}\right)^2 + Z_0^2\right] = 0.\end{aligned} \tag{9}$$

The coefficients of all terms with respect to ω have to be zero to satisfy (9) for all ω. We can then derive the determining condition as follows:

$$Z_0 = \sqrt{\frac{L_S}{C_P}} = \sqrt{\frac{L_P}{C_S}}. \tag{10}$$

Substituting (10) into (7) leads to

$$\phi = \pi. \tag{11}$$

As a result, it has been shown that only an 180° phase difference is obtained without frequency dependence by satisfying the determining condition of (10).

B. Non-180° Phase-Difference Case

Next, we derive the condition in the case of non-180° phase-difference ϕ_0 over a broad bandwidth. To yield a broad-band phase difference characteristics, it is required to satisfy conditions as follows :

$$\phi|_{\omega=\omega_1} = \phi|_{\omega=\omega_2} = \phi_0 \tag{12}$$

$$\left.\frac{d\phi}{d\omega}\right|_{\omega=\omega_1} = \left.\frac{d\phi}{d\omega}\right|_{\omega=\omega_2} = 0. \tag{13}$$

Substituting (7) into (12), we obtain the following equations:

$$\begin{aligned}&\frac{2Z_0\left(\omega_1 L_S - \dfrac{1}{\omega_1 C_S}\right)}{\left(\omega_1 L_S - \dfrac{1}{\omega_1 C_S}\right)^2 - Z_0^2} - \frac{2Z_0\left(\dfrac{1}{\omega_1 L_P} - \omega_1 C_P\right)}{1 - Z_0^2\left(\dfrac{1}{\omega_1 L_P} - \omega_1 C_P\right)^2} \\ &\quad = \tan\phi_0\end{aligned} \tag{14}$$

$$\begin{aligned}&\frac{2Z_0\left(\omega_2 L_S - \dfrac{1}{\omega_2 C_S}\right)}{\left(\omega_2 L_S - \dfrac{1}{\omega_2 C_S}\right)^2 - Z_0^2} - \frac{2Z_0\left(\dfrac{1}{\omega_2 L_P} - \omega_2 C_P\right)}{1 - Z_0^2\left(\dfrac{1}{\omega_2 L_P} - \omega_2 C_P\right)^2} \\ &\quad = \tan\phi_0.\end{aligned} \tag{15}$$

From (7) and (13), we obtain the following equations:

$$\begin{aligned}&\left(\omega_1 L_S + \frac{1}{\omega_1 C_S}\right)\left[1 + Z_0^2\left(\frac{1}{\omega_1 L_P} - \omega_1 C_P\right)^2\right] \\ &\quad = \left(\frac{1}{\omega_1 L_P} + \omega_1 C_P\right)\left[\left(\omega_1 L_S - \frac{1}{\omega_1 C_S}\right)^2 + Z_0^2\right]\end{aligned} \tag{16}$$

$$\begin{aligned}&\left(\omega_2 L_S + \frac{1}{\omega_2 C_S}\right)\left[1 + Z_0^2\left(\frac{1}{\omega_2 L_P} - \omega_2 C_P\right)^2\right] \\ &\quad = \left(\frac{1}{\omega_2 L_P} + \omega_2 C_P\right)\left[\left(\omega_2 L_S - \frac{1}{\omega_2 C_S}\right)^2 + Z_0^2\right].\end{aligned} \tag{17}$$

To reduce (14)–(17) to solvable forms, we introduce the conditions as follows:

$$\omega_1 = \frac{1}{\sqrt{L_S C_S}} \tag{18}$$

$$\omega_2 = \frac{1}{\sqrt{L_P C_P}} \tag{19}$$

$$\omega_C = \frac{\omega_1 + \omega_2}{2}. \tag{20}$$

Equation (18) corresponds to the condition that ϕ at ω_1 is the phase difference between the series circuit L_S/C_S as a short termination and parallel circuit L_P/C_P. Equation (19) corresponds to the condition that ϕ at ω_2 is the phase difference between the series circuit L_S/C_S and parallel circuit L_P/C_P as an open termination. The ω_C is the center frequency of ω_1 and ω_2.

We can then reduce (14) and (15) to the following equations:

$$\tan\phi_0 = -\frac{2Z_0\left(\frac{1}{\omega_1 L_P} - \omega_1 C_P\right)}{1 - Z_0^2\left(\frac{1}{\omega_1 L_P} - \omega_1 C_P\right)^2} \tag{21}$$

$$\tan\phi_0 = \frac{2Z_0\left(\omega_2 L_S - \frac{1}{\omega_2 C_S}\right)}{\left(\omega_2 L_S - \frac{1}{\omega_2 C_S}\right)^2 - Z_0^2}. \tag{22}$$

Equations (21) and (22) can be rewritten as follows:

$$Z_0^2 \tan\phi_0\left(\frac{1}{\omega_1 L_P} - \omega_1 C_P\right)^2 - 2Z_0\left(\frac{1}{\omega_1 L_P} - \omega_1 C_P\right) - \tan\phi_0 = 0 \tag{23}$$

$$\tan\phi_0\left(\omega_2 L_S - \frac{1}{\omega_2 C_S}\right)^2 - 2Z_0\left(\omega_2 L_S - \frac{1}{\omega_2 C_S}\right) - Z_0^2\tan\phi_0 = 0. \tag{24}$$

Finally, we obtain solvable forms of (14) and (15) as follows:

$$\frac{1}{\omega_1 L_P} - \omega_1 C_P = \left(\frac{1+\cos\phi_0}{\sin\phi_0}\right)\frac{1}{Z_0} \tag{25}$$

$$\omega_2 L_S - \frac{1}{\omega_2 C_S} = \left(\frac{1+\cos\phi_0}{\sin\phi_0}\right) Z_0. \tag{26}$$

We also reduce (16) and (17) to solvable forms as follows:

$$\omega_2 = \left[1 + \left(\frac{1+\cos\phi_0}{\sin\phi_0}\right)^2 + \left(\frac{1+\cos\phi_0}{\sin\phi_0}\right) \cdot \sqrt{2 + \left(\frac{1+\cos\phi_0}{\sin\phi_0}\right)^2}\right]\omega_1 \left(= A(\phi_0)\omega_1\right). \tag{27}$$

Let $A(\phi_0)$ be the coefficient of (27). From (20) and (27), ω_1 and ω_2 are expressed as follows:

$$\omega_1(\phi_0) = \frac{2}{A(\phi_0)+1}\,\omega_C \tag{28}$$

$$\omega_2(\phi_0) = \frac{2A(\phi_0)}{A(\phi_0)+1}\,\omega_C. \tag{29}$$

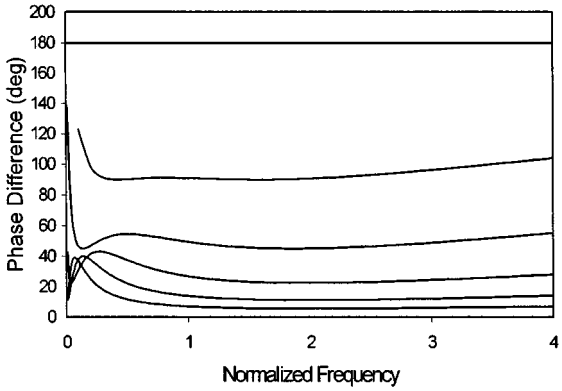

Fig. 3. Ideal phase-difference characteristics of the reflective terminating circuit.

The circuit elements L_S, C_S, L_P, and C_P are then given as follows:

$$L_S(\omega_C, \phi_0) = \frac{A(\phi_0)}{A(\phi_0)-1}\left(\frac{1+\cos\phi_0}{\sin\phi_0}\right)\frac{Z_0}{\omega_C} \tag{30}$$

$$C_S(\omega_C, \phi_0) = \frac{(A(\phi_0)-1)(A(\phi_0)+1)^2}{4A(\phi_0)}\left(\frac{\sin\phi_0}{1+\cos\phi_0}\right)\frac{1}{\omega_C Z_0} \tag{31}$$

$$L_P(\omega_C, \phi_0) = \frac{(A(\phi_0)-1)(A(\phi_0)+1)^2}{4A(\phi_0)^2}\left(\frac{\sin\phi_0}{1+\cos\phi_0}\right)\frac{Z_0}{\omega_C} \tag{32}$$

$$C_P(\omega_C, \phi_0) = \frac{1}{A(\phi_0)-1}\left(\frac{1+\cos\phi_0}{\sin\phi_0}\right)\frac{1}{\omega_C Z_0}. \tag{33}$$

Therefore, the circuit elements have been expressed as functions of ω_C and ϕ_0. Substituting (30)–(33) with (7), it is easily shown that ϕ is a function of ω/ω_C. The ideal phase-difference characteristics versus normalized frequency ω/ω_C are plotted in Fig. 3. In the case of a 90° phase difference, the phase-difference variation is less than 1.17° over ω_1 to ω_2, where ω_1 and ω_2 are $0.42\omega_C$ and $1.58\omega_C$, respectively.

III. Design

A. 180° Reflective-Terminating-Circuit MMIC

Fig. 4 shows a schematic diagram of the proposed 180° reflective terminating circuit. It consists of only a few circuit elements of built-in inductor L_b, built-in capacitor C_b, and a pair of FET1 and FET2. These FETs are used as switching elements.

Fig. 5 shows equivalent circuits of parallel and series *LC* states of the 180° reflective terminating circuit, respectively. R_{on1} and R_{on2} are the on-state resistances of FET1 and FET2, respectively. C_{off1} and C_{off2} are the off-capacitances of FET1 and FET2, respectively. In parallel *LC* state operation, FET1 and FET2 are turned on, as shown in Fig. 5(a). By neglecting R_{on1} and R_{on2}, the circuit can be simplified to a parallel *LC* circuit, which corresponds to the parallel resonant circuit of L_P/C_P in Fig. 2. In series *LC* state operation, FET1 and FET2 are pinched off, as shown in Fig. 5(b). When the admittance of a series capacitance combination consisting of C_b and C_{off2} is

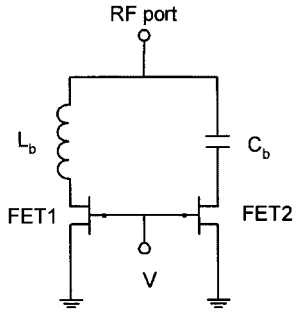

Fig. 4. Schematic diagram of proposed 180° reflective terminating circuit.

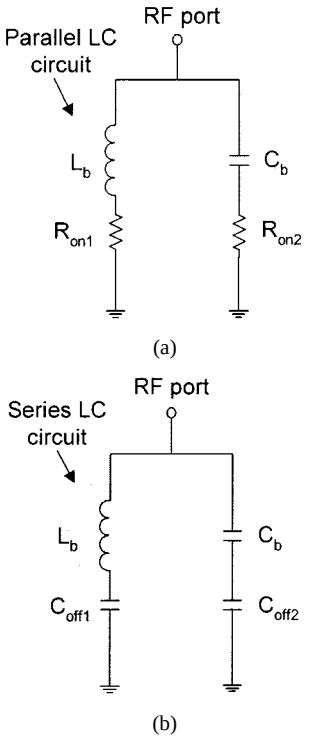

Fig. 5. Equivalent circuits of parallel and series *LC* states of 180° reflective terminating circuit. (a) Parallel *LC* state. (b) Series *LC* state.

small enough to be neglected, the circuit can be simplified to a series *LC* circuit, which corresponds to the series resonant circuit of L_s/C_s in Fig. 2. Therefore, Fig. 4 can be identical to Fig. 2 provided that L_b plays the role of L_P and L_S simultaneously. From (10), C_P, C_S, and $C_{\rm off1}$ must be equal to C_b. We have the determining condition for the circuit shown in Fig. 4. When the resonant frequency of the parallel and the series *LC* circuits is set to be ω_0, the circuit elements of L_b, C_b, and $C_{\rm off1}$ are determined uniquely as follows:

$$L_b = \frac{Z_0}{\omega_0} \tag{34}$$

$$C_b = C_{off1} = \frac{1}{\omega_0 Z_0}. \tag{35}$$

However, the parallel *LC* state has a return loss that is determined by nonzero $R_{\rm on1}$ and $R_{\rm on2}$. The return-loss increase in the parallel *LC* state particularly appears at ω_0. Therefore, the parasitic resistances of FETs place a constraint on the operating bandwidth. ω_0 has to be optimally determined larger than the operating bandwidth. From (34) and (35), the values of L_b and

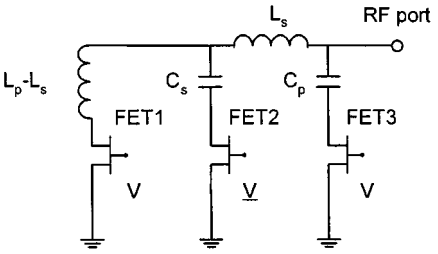

Fig. 6. Schematic diagram of a proposed 90° reflective terminating circuit.

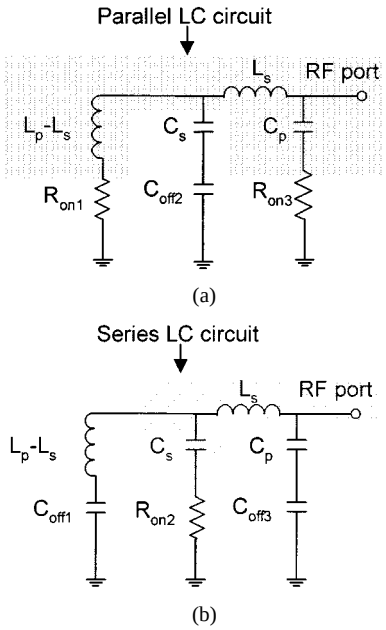

Fig. 7. Equivalent circuits of parallel and series *LC* states of 90° reflective terminating circuit. (a) Parallel *LC* state. (b) Series *LC* state.

C_b are 0.23 nH and 0.09 pF under the assumption of $Z_0 = 50\ \Omega$ and $\omega_0 = 2\pi \times 35$ GHz.

B. 90° Reflective Terminating Circuit MMIC

Fig. 6 shows a schematic diagram of a proposed 90° reflective terminating circuit. It consists of two inductors, two capacitors, and their FETs. These FETs are used as switching elements.

Fig. 7 shows equivalent circuits of parallel and series *LC* states of the 90° reflective terminating circuit, respectively. $R_{\rm on1}$, $R_{\rm on2}$, and $R_{\rm on3}$ are the on-state resistances of FET1, FET2, and FET3, respectively. $C_{\rm off1}$, $C_{\rm off2}$, and $C_{\rm off3}$ are the off-capacitances of FET1, FET2, and FET3, respectively. In parallel *LC* state operation, FET2 is pinched off and FET1 and FET3 are turned on, as shown in Fig. 7(a). In the condition that C_s, $C_{\rm off2}$, $R_{\rm on1}$, and $R_{\rm on3}$ can be neglected, the circuit can be simplified to a parallel *LC* circuit, which corresponds to the parallel resonant circuit of L_p/C_p in Fig. 2. In series *LC* state operation, FET1 and FET3 are pinched off and FET2 is turned on, as shown in Fig. 7(b). In the condition that C_p, $C_{\rm off3}$, $L_p - L_s$, $C_{\rm off1}$, and $R_{\rm on2}$ can be neglected, the circuit can be simplified to a series *LC* circuit, which corresponds to the series resonant circuit of L_s/C_s in Fig. 2. The FET size was determined so as to equalize the return loss of the series and parallel *LC* states due to small $R_{\rm on1}$, $R_{\rm on2}$, and $R_{\rm on3}$. From (30)–(33), the values of L_S, C_S, L_P, and C_P

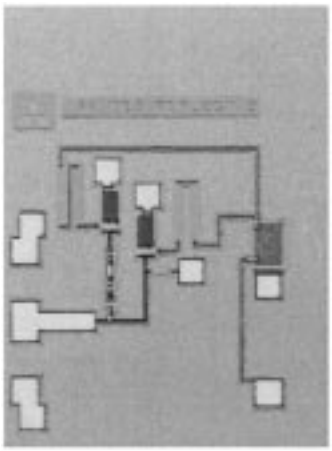

Fig. 8. Fabricated 180° reflective terminating circuit MMIC.

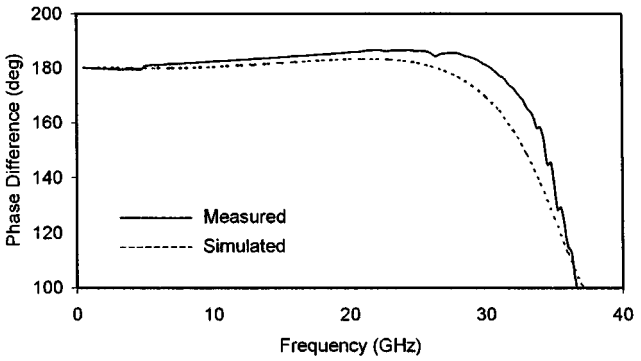

Fig. 9. Phase-difference performance of the 180° reflective terminating circuit MMIC.

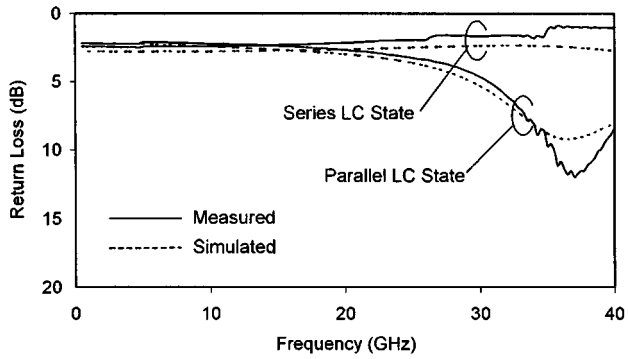

Fig. 10. Return-loss performance of the 180° reflective terminating circuit MMIC.

are 0.68 nH, 3.26 pF, 2.19 nH, and 0.073 pF, respectively, under the assumption of $Z_0 = 50\ \Omega$ and $\omega_C = 2\pi \times 8$ GHz. ω_S and ω_P are $2\pi \times 3.38$ GHz and $2\pi \times 12.6$ GHz, respectively.

IV. Measured Results

A. 180° Reflective Terminating Circuit and Phase-Shifter MMIC

Fig. 8 depicts a photograph of a fabricated 180° reflective terminating circuit MMIC. The integrated circuit (IC) has been fabricated by using 0.5-μm pHEMT technology. To equalize the return loss between parallel and series *LC* states, a resistor

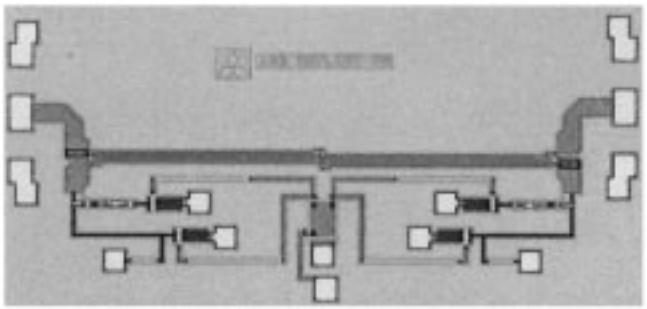

Fig. 11. 180° phase-shifter MMIC.

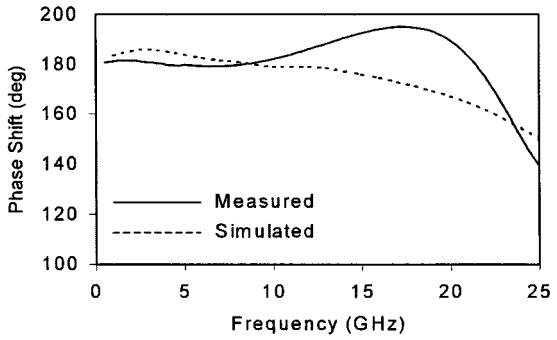

Fig. 12. Phase-shift performance of the 180° phase-shifter MMIC.

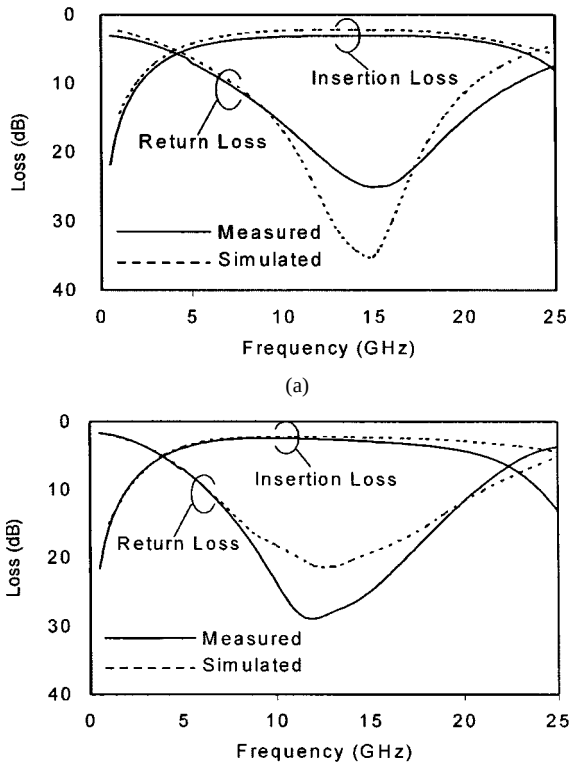

Fig. 13. Insertion- and return-loss performance of the 180° phase-shifter MMIC (a) Parallel *LC* state. (b) Series *LC* state.

is incorporated between source and drain terminals of FET1. That resistor has a negligible effect on phase difference and impedance of the circuit. Fig. 9 shows the simulated and measured phase-difference characteristics of the 180° reflective terminating circuit MMIC. Fig. 10 shows the return-loss

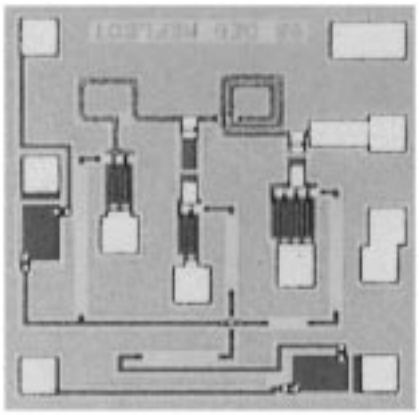

Fig. 14. Fabricated 90° reflective terminating circuit MMIC.

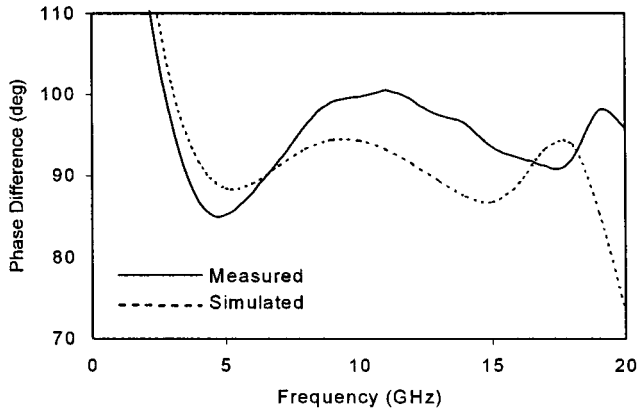

Fig. 15. Phase-difference performance of the 90° reflective terminating circuit MMIC.

characteristics. Both of the measured and simulated results are in good agreement. The measured phase difference is 183°±3° over 0.5–30 GHz, and the measured return loss is 2.3±0.4 dB over 0.5–20 GHz.

Fig. 11 presents an ultra-broad-band 180° reflection-type phase-shifter MMIC fabricated by the same process. It consists of a 3-dB Lange coupler and a pair of 180° reflective terminating circuits. Fig. 12 shows the measured and simulated phase-shift characteristics of the phase-shifter MMIC. Fig. 13 shows the measured and simulated loss characteristics. The measured phase shift is 187°±7° over 0.5–20 GHz. The measured insertion loss is 3.7±0.6 dB over 6–20 GHz and the measured insertion-loss error between parallel and series *LC* states is less than 1 dB at the same frequency range. The difference between the measured and simulated phase shift is mainly due to differences between the model parameter and measured data of a 3-dB Lange coupler used in it.

B. 90° Reflective Terminating Circuit MMIC

Fig. 14 depicts a photograph of a 90° reflective terminating circuit MMIC fabricated by the same process. Fig. 15 shows the simulated and measured phase-difference characteristics of the 90° reflective terminating circuit MMIC. Fig. 16 shows the return-loss characteristics. The measured phase difference is 93°±7° over 4–12 GHz, and the measured return loss is

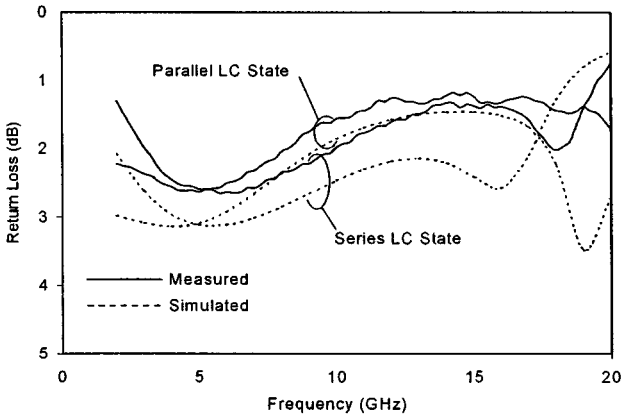

Fig. 16. Return-loss performance of the 90° reflective terminating circuit MMIC.

1.95±0.7 dB at the same frequency range. The difference between the measured and simulated phase difference are mainly caused by differences between the measured and simulated FET characteristics used in it.

V. Conclusions

We have presented an ultra-broad-band reflection-type phase shifter, which is composed of a broad-band 3-dB hybrid coupler and a pair of novel reflective terminating circuits. Theoretically, the proposed phase shifter has frequency-independent characteristics in the case of a 180° phase shift. The reflective terminating circuit switches two states of series and parallel *LC* circuits. Using an ideal circuit model without parasitic circuit elements, we have derived the determining condition of circuit elements for frequency independence. Extending the concept, we can also obtain a broad-band phase shifter for other phase differences as well. For a given phase difference and an operating frequency, we also have derived a condition to obtain minimum variation of phase difference around the operating frequency. The fabricated 180° reflective terminating circuit MMIC has achieved a phase difference of 183°±3° over 0.5–30 GHz. The fabricated 180° phase-shifter MMIC utilizing the reflective terminating circuits has successfully demonstrated a phase shift of 187°±7° over 0.5–20 GHz. The fabricated 90° reflective terminating circuit MMIC has performed a phase difference of 93°±7° over 4–12 GHz.

References

[1] R. V. Garver, "Broad-band diode phase shifters," *IEEE Trans. Microwave Theory Tech.*, vol. MTT-20, pp. 314–323, May 1972.

[2] J. P. Starski, "Optimization of the matching network for a hybrid coupler phase shifter," *IEEE Trans. Microwave Theory Tech.*, vol. MTT-25, pp. 662–666, Aug. 1977.

[3] M. Schindler, Y. Ayasli, A. Morris, and L. Hanes, "Monolithic 6–18 GHz 3-bit phase shifter," in *IEEE GaAs IC Symp. Dig.*, 1985, pp. 129–132.

[4] D. C. Boire, J. E. Dejenford, and M. Cohn, "A 4.5 to 18 GHz phase shifter," in *IEEE MTT-S Int. Microwave Symp. Dig.*, 1985, pp. 601–604.

[5] D. C. Boire, G. St. Onge, C. Barratt, G. B. Norris, and A. Moysenko, "4:1 bandwidth digital five bit MMIC phase shifters," in *IEEE Microwave Millimeter-Wave Monolithic Circuits Symp. Dig.*, 1989, pp. 69–73.

[6] H. A. Atwater, "Reflection coefficient transformations for phase-shift circuits," *IEEE Trans. Microwave Theory Tech.*, vol. MTT-28, pp. 563–567, June 1980.

Kenichi Miyaguchi (M'00) received the B.E. and M.E. degrees in electrical and electronic engineering from Kyoto University, Kyoto, Japan, in 1997 and 1999, respectively.

In 1999, he joined the Information Technology Research and Development Center, Mitsubishi Electric Corporation, Kamakura, Japan, where he has been engaged in research and development of microwave control circuits and MMICs.

Mr. Miyaguchi is a member of the Institute of Electronics, Information and Communication Engineers (IEICE), Japan.

Morishige Hieda (M'94) was born in Toyoma, Japan. He received the B.E. and M.E. degrees in electronic engineering from Tohoku University, Sendai, Japan, in 1988 and 1990, respectively.

In 1990, he joined the Information Technology Research and Development Center, Mitsubishi Electric Corporation, Kamakura, Japan, where he has been engaged in research and development of millimeter-wave mixers, microwave control circuits, and MMICs.

Mr. Hieda is a member of the Institute of Electronics, Information and Communication Engineers (IEICE), Japan.

Kazuhiko Nakahara (M'01) received the B.S. and Ph.D. degrees in electronics from Hokkaido University, Sapporo, Japan, in 1983 and 2001, respectively.

In 1983, he joined the Mitsubishi Electric Corporation, Kamakura, Japan, where he was engaged in research and development of microwave ICs and MMICs. He is currently with Kamakura Works, Mitsubishi Electric Corporation, Kamakura, Japan.

Dr. Nakahara is a member of the Institute of Electronics, Information and Communication Engineers (IEICE), Japan.

Hitoshi Kurusu received the B.E. and M.E. degrees in electrical and electronic engineering from Kyoto University, Kyoto, Japan, in 1994 and 1996, respectively.

In 1996, he joined the High Frequency and Optical Semiconductor Division, Mitsubishi Electric Corporation, Itami, Japan, where he has been engaged in research and development of microwave control circuits and MMICs.

Masatoshi Nii received the B.E. and M.E. degrees in electronic and electrical engineering from Fukuoka University, Fukuoka, Japan, in 1989 and 1991, respectively.

In 1991, he joined the Communication Systems Center, Mitsubishi Electric Corporation, Amagasaki, Japan, where he has been engaged in the development of microwave modules, microwave circuits, and MMICs.

Mr. Nii is a member of the Institute of Electronics, Information and Communication Engineers (IEICE), Japan.

Michiaki Kasahara received the B.E. degree in electrical engineering from the University of Electro-Communications, Tokyo, Japan, in 1985.

In 1985, he joined the Information Technology Research and Development Center, Mitsubishi Electric Corporation, Kamakura, Japan, where he has been engaged in development of RF equipment for radar systems

Mr. Kasahara is a member of the Institute of Electronics, Information and Communication Engineers (IEICE), Japan.

Tadashi Takagi (M'92) received the B.S. degree in physics from the Tokyo Institute of Technology, Tokyo, Japan, in 1973, and Ph.D. degree in electronic engineering from Shizuoka University, Sizuoka, Japan, in 1995.

In 1973, he joined the Mitsubishi Electric Corporation, Kamakura, Japan, where he was engaged in research and development of microwave circuits and MMICs and solid-state power amplifiers (SSPAs). He is currently the Project Manager of the Microwave Prototyping Project Group, Information Technology Research and Development Center, Mitsubishi Electric Corporation.

Dr. Takagi is a member of the Institute of Electronics, Information and Communication Engineers (IEICE), Japan.

Shuji Urasaki (M'82–SM'94) received the B.S., M.S., and Ph.D. degrees in electronic engineering from Hokkaido University, Sapporo, Japan, in 1967, 1969, and 1985, respectively.

In 1969, he joined the Mitsubishi Electric Corporation, Tokyo, Japan, where he was involved with antennas for public communications, satellite communications, and radar systems. He is currently the General Manager of the Electro-Optics and Microwave Systems Laboratory, Information Technology Research and Development Center, Mitsubishi Electric Corporation, Kamakura, Japan.

Dr. Urasaki is a member of the Institute of Electronics, Information and Communication Engineers (IEICE), Japan.